Exposure and Health (2024) 16:291–306
https://doi.org/10.1007/s12403-023-00555-y

ORIGINAL PAPER

# Hydrogeochemical Processes Regulating the Groundwater Geochemistry and Human Health Risk of Groundwater in the Rural Areas of the Wei River Basin, China

**Wenyu Guo[1,2,3] · Peiyue Li[1,2,3] · Qianqian Du[1,2,3] · Yuhan Zhou[1,2,3] · Duoxun Xu[4] · Ziying Zhang[5]**

Received: 29 January 2023 / Revised: 20 February 2023 / Accepted: 3 April 2023 / Published online: 17 April 2023


**Abstract**

The hydrochemical characteristics of phreatic water were evaluated in this study, and the hydrogeochemical processes occurring along groundwater flow paths were analyzed using inverse hydrogeochemical simulations. The spatial distributions of groundwater Fe and Mn contents in the study area, their influencing factors, and their correlative probabilistic human health risks were assessed. The results showed that the order of cation content in phreatic water was $Ca^{2+} > Mg^{2+} > Na^{+} > K^{+}$ and $Ca^{2+} > Na^{+} > Mg^{2+} > K^{+}$ in the pluvial-alluvial fan and alluvial plain, respectively. Approximately 92.73% of the phreatic water samples were $HCO_3$-Ca·Mg-type water, and only a few belonged to $SO_4$·Cl-Ca·Mg-type water. Twelve percent and forty percent of the phreatic water in the pluvial-alluvial fan and alluvial plain, respectively, showed Fe and Mn concentrations exceeding China's drinking water standards. Hydrogeochemical simulations using PHREEQC showed some differences in water−rock interactions between paths and along the same path due to differences in lithological and hydrological conditions. In addition, higher Fe and Mn contents mainly occurred in the Huyi District, as well as in some parts of the alluvial plain aquifer. Moreover, groundwater Fe and Mn contents were mainly influenced by redox potential, infiltration of sewage containing high Fe and Mn concentrations, TDS contents, and groundwater flow rates. In the Wei River basin, the probability of the health risk due to $NO_3$-N, Fe, and Mn was ordered as $NO_3$-N > Mn > Fe. The health risks of $NO_3$-N were 3.1% and 18.3% for adults and children, respectively, and the health risks due to Mn were 2.3% and 4.9% for adults and children, respectively. In contrast, the probability of health risk of Fe was negligible.

**Keywords** Hydrogeochemistry · Groundwater quality · Hydrogeochemical simulation · Semiarid area · Wei River Basin

## Introduction

Groundwater is not only an important natural resource for human survival and development but also an important element involved in maintaining the ecological balance (Schlager 2006; Zhang et al. 2017). However, the amount of groundwater resources often does not meet the requirements for sustainable local and regional economic development, especially in arid and semiarid regions (Banerjee et al. 2016; Li et al. 2019a; Fathy et al. 2021). In addition, phreatic water contamination by nitrate ($NO_3^-$), organic matter, and heavy metals due to anthropogenic disturbances has often been overlooked in economic development over the past decades, resulting in groundwater contamination by nitrate ($NO_3^-$), organic matter, and heavy metals (e.g., Fe and Mn) and, consequently, accentuating the conflict between groundwater availability

✉ Peiyue Li
lipy2@163.com; peiyueli@chd.edu.cn

1 School of Water and Environment, Chang'an University, No. 126 Yanta Road, Xi'an 710054, Shaanxi, China

2 Key Laboratory of Subsurface Hydrology and Ecological Effects in Arid Region of the Ministry of Education, Chang'an University, No. 126 Yanta Road, Xi'an 710054, Shaanxi, China

3 Key Laboratory of Eco-Hydrology and Water Security in Arid and Semi-Arid Regions of the Ministry of Water Resources, Chang'an University, No. 126 Yanta Road, Xi'an 710054, Shaanxi, China

4 Xi'an Center of Mineral Resources Survey, China Geological Survey, No. 66 West Fengqi Road, Xi'an 710010, Shaanxi, China

5 Taizhou Vocational and Technical College, No. 788 Xueyuan Road, Taizhou 318000, Zhejiang, China

and sustainable socioeconomic development (Kurwadkar 2019; He et al. 2020; Wei et al. 2022).

Several studies have shown that high concentrations of contaminants in groundwater have great negative influences on human health and ecosystem components (Li et al. 2014a; Touhari et al. 2015; He et al. 2020). High Fe concentrations in drinking water can cause liver damage, joint pain, and fatigue (Yadav et al. 2019), while high Mn concentrations can cause some neurological disorders and increase infant mortality (Hafeman et al. 2007; Rutchik et al. 2012). Moreover, high $SO_4^{2-}$ and $NO_3^-$ concentrations pose high health risks to humans (Wu and Sun 2016). In recent years, human health risks in groundwater due to high contaminant concentrations have been widely investigated and have received extensive attention from governments and scholars. Zhang et al. (2019a) showed that the groundwater arsenic-associated cancerogenic risk for adults in the Jinghui irrigation district was 3.5 times higher than the national acceptable risk level. Snousy et al. (2022) revealed that high groundwater $SO_4^{2-}$ contents in Assiut District have serious harmful effects on human skin, hair, and eyes. Chakraborty et al. (2022) showed that water contamination by heavy metals poses a noncancerous health risk to the inhabitants of the Chotanagpur Plateau fringe of India. The sources of high anion and cation contents in groundwater are classified as natural and anthropogenic. For example, high $NO_3^-$ concentrations are often derived from anthropogenic factors, including agricultural fertilization and industrial effluent discharge (Wu and Sun 2016), while high groundwater $F^-$ concentrations are often caused by natural factors, such as evaporation and rock weathering (Chen et al. 2021). Heavy metal contents in groundwater may also be controlled by natural elements, such as groundwater-reducing environments (Kshetrimayum and Hegeu 2016). Therefore, the exploration of hydrogeochemical processes that influence the evolution of groundwater chemistry is especially vital to accurately identify the sources of groundwater chemical elements as well as the factors controlling their distribution and transport. Numerous studies on groundwater hydrogeochemistry have been carried out worldwide. Indeed, most of these studies have mainly focused on the sources and influences of water chemical composition, typical element enrichment in groundwater, quantitative simulation of hydrogeochemical processes, and impacts of groundwater level changes on groundwater chemistry evolution (Li et al. 2013, 2021; Jha et al. 2015; Singh et al. 2018; Su et al. 2020; Natesan et al. 2022). The results of some studies indicate that hydrodynamic conditions, topography and lithological stratigraphy, the intensity of water–rock interactions, and circulation conditions lead to the zonation of groundwater chemical characteristics in the horizontal direction (Jing et al. 2014; Dragon et al. 2009).

The Wei River Basin is a typical water shortage area, and groundwater is an important support for the development of agriculture, industry, and water supply for residents in the area. Especially, in the vast rural areas, phreatic water is an important source of water supply. Most of the wells are located in the pluvial-alluvial fan area in front of the mountain, and the particles in the pluvial-alluvial fan area are coarse, so the groundwater quality can be very easily polluted. However, due to the lack of attention to the groundwater pollution problem, phreatic water pollution in the Wei River Basin is serious, which also induced water pollution in confined groundwater in some areas. Previous studies have highlighted groundwater pollution in the Wei River Basin, including $NO_3^-$, $F^-$, and heavy metal (As, Fe, and Mn) pollution due to the influences of anthropogenic factors (Ren et al. 2021; Guo et al. 2022; Wang et al. 2022). These issues restrict the sustainable use and effective management of local groundwater resources and threaten the safe supply of groundwater in the Wei River Basin. In recent years, several research teams have investigated the hydrochemical processes at different scales in the Wei River basin. Xu et al. (2019) studied the hydrogeochemical characteristics of the entire Wei River basin and clarified that the controlling factors of groundwater chemistry are different in the north and south of the Wei River. Zhang et al. (2020a) studied the characteristics of groundwater chemistry influenced by irrigation and the influence of hydrogeochemical processes on fluorine enrichment. Chen et al. (2021) explored the influence of groundwater chemistry and hydrogeochemical processes on groundwater fluoride throughout the Guanzhong Plain. Previous studies have shown that geological features and groundwater flow direction affect groundwater hydrochemical and hydrogeochemical processes (Ma et al. 2018; Poetra et al. 2020). Therefore, studying the hydrochemical characteristics of groundwater in different geomorphological zones and revealing the hydrogeochemical processes along the groundwater flow direction in the Wei River basin are important to clarify the fate of contaminants.

Moreover, $NO_3^-$, Fe, and Mn have been identified typical contaminants of groundwater in the Wei River Basin. $NO_3^-$ pollution in this area has been well researched by Xu et al. (2023). They also assessed the health risk caused by ingestion of high $NO_3^-$ groundwater using deterministic methods. However, the high Fe and Mn contents in groundwater are often overlooked. The Fe and Mn contents in groundwater at several water supply sources in Xi'an exceed the drinking water quality standards. The main factors influencing the distribution and enrichment of Fe and Mn in phreatic water remain unclear. In this context, the objectives of this study are (1) to assess the hydrochemical characteristics of the phreatic water and reveal the hydrogeochemical processes controlling groundwater chemistry in the Wei River Basin through reverse simulations via PHREEQC,

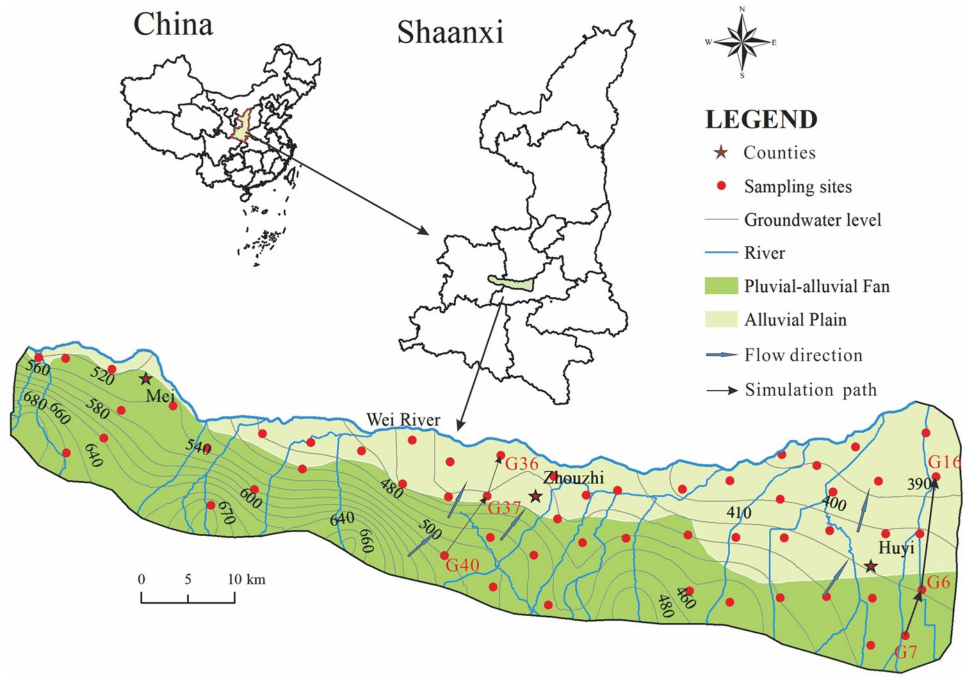


**Fig. 1** Location of the study area and sampling sites

(2) to identify the main variables influencing the abundance and enrichment of Fe and Mn in groundwater, and (3) to assess the probability of human health risks associated with Fe, Mn, and $NO_3^-$ in phreatic water.

## Study Area

### Geographic Location and Climatic Characteristics

The study area is situated in the southern Wei River Basin, Shaanxi Province, China. The surface elevation in the study area decreases gradually from the southern part to the northern part (Fig. 1). The study area is characterized by a warm-temperate semiarid and semihumid continental monsoon climate, with an average annual temperature, average annual precipitation, and average annual evaporation of 12–14 °C, 745.8 mm, and 700–1200 mm, respectively. Indeed, approximately 70–80% of the annual precipitation occurs mainly during the summer and autumn seasons, while the highest evaporation rates are observed mainly in July (Xu et al. 2023). The study area has a dense network of rivers, all of which originate in the northern Qinling Mountains. However, although the river network is dense, its flow rates are relatively low, flowing into the Wei River (Zhang et al. 2013). The Shitou, Lao, Feng, and Hei Rivers are large rivers that all cover a total area over 500 km$^2$. The regional landform genesis may be grouped into pluvial-alluvial fan and alluvial plain. The pluvial-alluvial fan is mainly located at the front of the Qinling Mountains and consists of multiphase pluvial-alluvial fans. The pluvial-alluvial fans in front of the Qinling Mountains are distributed in Mei County-Zhouzhi County-Huyi District, sloping toward the northern part and consisting of fine soil particles and a large thickness. The alluvial plain of the Wei River and its tributaries is created by the river flows of the Wei River and its tributaries, such as the Ba River, Lao River, Feng River, Hei River, and Shitou River.

The three districts and counties covered by the study area include Huyi District, Zhouzhi County, and Mei County, which belong to the major regions of China's western development. Groundwater resources including phreatic water and confined groundwater are the main source of water supply in the Wei River Basin, accounting for more than 40% of the total water supply. Groundwater is, therefore, critical for sustainable socioeconomic development in the Wei River Basin.

### Hydrogeological Characteristics

Groundwater in the Wei River Basin circulates mainly in Quaternary, Neogene, and Paleogene aquifers. Among them, the Quaternary aquifer is approximately 800 m thick, of which the lithological classes consist of loess, sand, and gravel layers, providing a good yield range of 50–200 m$^3$/h. The Neogene and Paleocene aquifers are approximately several kilometers thick, consisting mainly of mudstone and medium- to fine-grained sandstone, cemented and loose sandstone, and fractured bedrock, providing a good yield range of 30–80 m$^3$/h.

The aquifer in the study area is continuously distributed over the entire basin. The water-bearing group in the study area can be divided into a confined water-bearing group and a phreatic water-bearing group. The confined aquifer is composed of sandy pebbles, medium coarse, and fine sands and subsandy soils with alternating alluvial and flooding sediments. The phreatic aquifer in the study area can be divided into pore water in the pluvial-alluvial fan and pore water in the alluvial plain. The phreatic water in the alluvial plain is distributed in the terraces of the Wei River. The aquifer consists generally of sand, gravel pebbles, and sandy clay layers from the middle Pleistocene to Holocene with a thickness range of 5–80 m. However, phreatic water in the pluvial-alluvial fan is mainly distributed in the southern part of the Wei River Basin, of which the water-bearing layer consists mainly of gravel pebbles, drift stone, and sandy clay. Indeed, the water richness at the fan axis of the pluvial-alluvial fan is better than that between fans, while those at the middle and front edges are better than that of the trailing edge. The water abundance of the middle and front edges of the pluvial-alluvial fan is better than that at the rear edge, while the water abundance is better in the newly formed pluvial-alluvial fan than in the loess-covered pluvial-alluvial fan.

The phreatic water level depth ranges from 0.97 to 71.30 m and gradually decreases from south to north. Sediment particles of the middle and Cenozoic clastic rocks change from coarse to fine from the edges to the Wei River Basin central area. Precipitation, river infiltration, and lateral flows from the fronts of the Qinling Mountains are the primary phreatic water recharge sources in the alluvial plain (Li et al. 2016a). In contrast, the groundwater recharge in front of the Qinling Mountains mainly originates from precipitation infiltration. Evaporation, horizontal discharge to the Wei River, and artificial abstractions are the dominant methods of discharge in the Wei River Basin.

## Material and Methods

### Sample Collection and Hydrochemical Analysis

Fifty-five phreatic water samples were collected in July 2021 (Fig. 1). The groundwater level depth divers from one place to another, ranging within 0.92−42.5 m. Sampling and preservation of water samples were carried out according to the Technical specifications for environmental monitoring of groundwater (Ministry of Environmental Protection of the P. R. China 2020). The well water was extracted for 10–15 min before sampling. After rinsing the bottles with the groundwater to be collected for 2–3 times, all groundwater samples were collected in white polyethylene bottles with appropriate protective agents. The containers were sealed and labeled immediately after collection of the water samples. The samples were stored in a refrigerated environment at 4 °C and sent for testing within one week. The water samples were tested according to Chinese drinking water standards (Standardization Administration of the People's Republic of China 2006). The oxidation−reduction potential (ORP), electrical conductivity (EC), temperature (T), and pH of the phreatic water were measured in situ. Major cations ($Ca^{2+}$, $Mg^{2+}$, $Na^{+}$, and $K^{+}$), anions ($HCO_3^{-}$, $Cl^{-}$, $SO_4^{2-}$, and $NO_3^{-}$), trace elements ($F^{-}$, Fe, Mn, and As), and TDS were analyzed in the laboratory. The major cations ($Na^{+}$, $K^{+}$, $Ca^{2+}$, and $Mg^{2+}$) and Fe were analyzed using inductively coupled plasma atomic emission spectroscopy (ICP−AES). The analyses of $NO_3^{-}$, $SO_4^{2-}$, $F^{-}$, and $Cl^{-}$ were carried out using ion chromatography, while $HCO_3^{-}$ was measured by the acid–base titration method. Mn and As were measured by atomic absorption spectrophotometry and spectrophotometry, respectively. The TDS and TH contents were determined using the gravimetric and EDTA titration methods, respectively. The detection limits for $Ca^{2+}$, $Mg^{2+}$, $Na^{+}$, $K^{+}$, $HCO_3^{-}$, $Cl^{-}$, $SO_4^{2-}$, and $NO_3^{-}$ are 0.12, 0.05, 0.02, 0.003, 5.0, 0.007, 0.018, and 0.064 mg/L, respectively, while the detection limits for $F^{-}$, Fe, Mn, and As are 0.006, 0.02, 0.0048, and 0.0008 mg/L, respectively. The ion equilibrium error percentages were calculated for all groundwater samples, showing detection errors within $\pm 10\%$, which is acceptable for general hydrochemical studies.

## Methods

### Hydrogeochemical Modeling

The PHREEQC software developed by the U.S. Geological Survey (USGS) was used in this study to simulate the saturation index (SI) and hydrogeochemical processes of phreatic water in the southern part of the Wei River Basin. Indeed, the value of SI can determine whether minerals in the water are in a saturation or undersaturation state according to the following formula:

$$SI = \lg \frac{IAP}{K} \tag{1}$$

where IAP denotes the ion activity product and $K$ is the equilibrium constant of the mineral dissolution reaction. $SI > 0$, $SI = 0$, and $SI < 0$ indicate that the mineral is in supersaturated, equilibrium, and unsaturated states, respectively, in the water sample.

In this study, hydrogeochemical inverse modeling in PHREEQC software was used to invert the possible water−rock reactions based on the hydrochemical data of groundwater at the initial and end points of the flow path to identify the complex reaction conditions occurring between groundwater and different minerals and gases and to quantify the extent to which water−rock interaction occurs (Li et al. 2010).

The reaction path of the reverse geochemical simulation requires that the starting and ending water samples are in the same flow path. Based on the hydrochemical data of groundwater, two paths were selected in this study to simulate the hydrogeochemical processes from the recharge area (Qinling Mountains) to the discharge area (Wei River) by considering water–rock interactions with fast and slow phreatic water flow rates. The simulation paths are shown in Fig. 1. The possible mineral phases were selected in this study based on previous research results and the lithological characteristics of the aquifer in the Wei River Basin (Guo et al. 2022), which were gypsum, calcite, dolomite, halite, illite, quartz, fluorite, albite, hematite, siderite, and pyrolusite. In addition, considering the extensive carbonic acid equilibrium and cation exchange in the submerged aquifer of the Wei River Basin, the cation exchange between $Ca^{2+}$, $Mg^{2+}$, $Na^{+}$, and $CO_2$(g) was also considered in the selected mineral phases.

## Health Risk Assessment Based on Monte Carlo Simulation

Human health risk assessment models can determine pollutant-related potential human health risks in groundwater. We used the model suggested in the Technical Guide for Risk Assessment of Contaminated Sites to assess the non-carcinogenic risk of Fe and Mn to local residents in this research (Ministry of Environmental Protection of the P.R. China 2019). The non-carcinogenic risk of pollutants to humans is expressed as a hazard quotient (HQ), which can be calculated using Eq. (2). HQ values higher than 1 suggest human health risks. Only health risk through drinking water intake was considered in this study, since health risk from other pathways is negligible (Wu et al. 2020).

$$HQ = \frac{Intake}{RfD} \tag{2}$$

where *RfD* denotes the reference dose of Fe, Mn and $NO_3$-N by drinking, which was set to 0.3, 0.02, and 1.6 (mg/kg·day) for Fe, Mn, and $NO_3$-N, respectively (Magesh et al. 2017). *Intake* denotes the exposure of humans to pollutants through water intake (mg/kg·day), which was calculated in this study according to the following formula:

$$Intake = \frac{C \times GWCR \times EF \times ED}{W \times T} \tag{3}$$

where all the definitions of the parameters in Eq. (2) are reported in Table 1.

Previous studies on health risk assessment have set each exposure parameter of Eq. (3) as a certain definite value. However, there are some uncertainties in the parameter values, including groundwater consumption rates, exposure frequencies, and body weight, due to the differences in environmental characteristics, geographical characteristics, and living habits (Ganyaglo et al. 2019), causing uncertainty in the health risk evaluation results. Therefore, traditional health risk evaluations have certain limitations and cannot comprehensively assess pollutant-related human health risks (Liu et al. 2022).

Monte Carlo computational methods can simulate the uncertainty of events through mathematical statistics and random sampling. The basic steps of this method are as follows: (1) establish the probability distribution of uncertainties; (2) use the uncertainties as factors from which the simulation tests are randomly sampled as the sampling values of the variable sequences; and (3) use the results of the simulation tests to obtain the simulated values at different confidence levels to derive the simulation results of uncertainty analysis. Indeed, several studies (Liu et al. 2022) have demonstrated the applicability of the Monte Carlo method in health risk evaluation. Therefore, the Monte Carlo method was chosen in this study to determine the distribution type of each parameter used in Eq. (3), considering the uncertainty of the GWCR, EF, and W parameters in the model. The final probability distribution results were obtained using Crystal Ball risk simulation software by performing 10,000 iterations of stochastic simulations for the non-carcinogenic risks for people in different age groups. The procedures of health risk assessment based on the Monte Carlo method are briefly shown in Fig. 2.

**Table 1** Parameter values for health risk estimation

| Parameters | Meaning of parameters | Units | Distribution types | Age groups | |
|---|---|---|---|---|---|
| | | | | Adults | Children |
| GWCR | Groundwater consumption rate | L/day | Normal | (1.5, 0.5) | (0.85, 0.09) |
| EF | Exposure frequency | day/year | Triangular | (180, 365, 345) | (180, 365, 345) |
| C | Contaminant concentration in groundwater | mg/L | Lognormal | – | – |
| ED | Exposure duration | year | – | 30 | 6 |
| W | Average weight | kg | Lognormal | (61.75, 6.18) | (15.00, 1.50) |
| T | Average effect time | day | – | 30 × 365 | 6 ×365 |

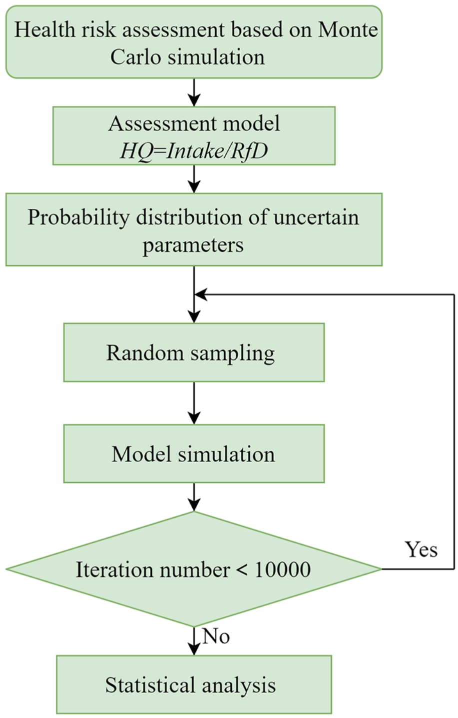


**Fig. 2** Procedure of health risk assessment based on the Monte Carlo simulation

The values and distribution types of exposure parameters for different groups were determined in this study based on previous related studies on health risk assessment in the Wei River Basin (Zhang et al. 2019b) and are reported in Table 1.

## Results and Discussion

### Hydrochemical Characteristics

The hydrochemical results of groundwater in the Wei River Basin in July 2021 are reported in Table 2. The pH values of groundwater in the study area ranged from 6.83 to 7.63 and 7.16 to 7.86, with average values of 7.33 and 7.49 in the pluvial-alluvial fan and alluvial plain, respectively. The TDS content ranges in groundwater of the pluvial-alluvial fan and alluvial plain were 264–1298 mg/L and 262–2566 mg/L, with average contents of 612.08 and 768.80 mg/L, respectively. The obtained results revealed a substantial increase in the mean TDS content from the pluvial-alluvial fan to the alluvial plain, which might be due to mineral dissolution in the submerged aquifer along the groundwater flow directions, as well as the potential influence of human activities (Li et al. 2016b).

The average major anion and cation contents in the alluvial plain located downstream of groundwater flow were

**Table 2** Statistical values of groundwater chemical parameters

| Index | Pluvial-alluvial fan ($n=25$) | | | | | Alluvial plain ($n=30$) | | | | |
|---|---|---|---|---|---|---|---|---|---|---|
| | Min | Max | Mean | SD | CV/% | Min | Max | Mean | SD | CV/% |
| pH | 6.83 | 7.63 | 7.33 | 0.21 | 2.80 | 7.16 | 7.86 | 7.49 | 0.20 | 2.66 |
| ORP | 154.00 | 237.00 | 192.00 | 22.42 | 11.73 | -107 | 214 | 130 | 89.46 | 68.57 |
| TDS | 264.00 | 1298.00 | 612.08 | 284.19 | 46.43 | 262 | 2566 | 768.80 | 415.36 | 54.03 |
| TH | 188.00 | 599.00 | 361.04 | 126.70 | 35.09 | 178 | 1191 | 457.30 | 196.85 | 43.05 |
| $Na^+$ | 4.83 | 38.10 | 15.38 | 8.65 | 56.27 | 11.8 | 308 | 46.62 | 53.30 | 114.33 |
| $K^+$ | 0.64 | 4.24 | 2.16 | 1.00 | 46.04 | 0.48 | 6.68 | 2.38 | 1.29 | 54.14 |
| $Ca^{2+}$ | 55.20 | 205.00 | 115.48 | 43.12 | 37.34 | 61.6 | 220 | 131.64 | 42.29 | 32.12 |
| $Mg^{2+}$ | 9.19 | 49.10 | 22.22 | 9.27 | 41.70 | 10.5 | 161 | 37.26 | 27.95 | 75.02 |
| $Cl^-$ | 2.60 | 96.10 | 22.08 | 19.21 | 86.98 | 6.09 | 210 | 40.66 | 37.80 | 92.97 |
| $SO_4^{2-}$ | 6.13 | 176.00 | 63.14 | 40.16 | 63.60 | 11.9 | 997 | 141.58 | 174.64 | 123.35 |
| $NO_3$-N | 2.24 | 89.65 | 27.11 | 22.97 | 84.72 | 0.01 | 70.68 | 18.48 | 19.07 | 103.21 |
| $HCO_3^-$ | 125.00 | 350.00 | 236.08 | 67.31 | 28.51 | 167 | 642 | 328.43 | 111.09 | 33.82 |
| F | 0.04 | 0.27 | 0.13 | 0.07 | 53.00 | 0.05 | 0.44 | 0.20 | 0.11 | 53.87 |
| Fe | 0.01 | 1.80 | 0.19 | 0.43 | 224.44 | 0.01 | 9.60 | 0.84 | 2.03 | 242.10 |
| Mn (μg/L) | 0.24 | 462.00 | 34.02 | 106.47 | 312.95 | 0.24 | 1417 | 155.92 | 301.31 | 193.24 |
| As (μg/L) | 1.46 | 3.01 | 2.13 | 0.41 | 19.28 | 7.16 | 7.86 | 7.49 | 0.20 | 2.66 |
| Calcite | − 0.82 | 0.71 | 0.17 | — | — | 0.06 | 0.9 | 0.51 | — | — |
| Dolomite | − 2.19 | 0.88 | − 0.12 | — | — | − 0.19 | 1.54 | 0.70 | — | — |
| Fluorite | − 3.57 | − 1.82 | − 2.69 | — | — | − 3.38 | − 1.53 | − 2.34 | — | — |
| Gypsum | − 2.8 | − 1.14 | − 1.79 | — | — | − 2.33 | − 0.61 | − 1.49 | — | — |

Unless otherwise marked, the units of Min, max, Mean and SD in the table are mg/L except for pH, ORP, calcite, dolomite, fluorite and gypsum higher than those in the upstream pluvial-alluvial fan. Indeed, $Ca^{2+}$ showed the highest cation contents in the phreatic water of the pluvial-alluvial fan, with an average concentration of 115.48 mg/L, and the content of $Mg^{2+}$ in the pluvial-alluvial fan was second only after $Ca^{2+}$, with an average concentration of 22.22 mg/L. $K^+$ displayed the lowest cation concentrations, with an average concentration of 2.16 mg/L. Similar results were observed in the alluvial plain in the southern part of the Wei River, showing average $Ca^{2+}$ and $K^+$ concentrations of 131.64 and 2.38 mg/L, respectively. The $Na^+$ concentrations in the alluvial plain were higher than those of $Mg^{2+}$, indicating average concentrations of 46.62 and 37.26 mg/L, respectively, which was probably caused by halite dissolution and cation exchange along the phreatic water flow directions. In the pluvial-alluvial fan, the average $Cl^-$, $SO_4^{2-}$, and $HCO_3^-$ concentrations were 22.08, 63.14, and 236.08 mg/L, respectively. The average $Cl^-$, $SO_4^{2-}$, and $HCO_3^-$ concentrations in the alluvial plain near the Wei River were 40.66, 141.58, and 328.43 mg/L, respectively.

Groundwater $NO_3^-$ pollution is a common environmental issue in the Wei River basin due mainly to intensive industrial and agricultural activities (Zhang et al. 2019c). The $NO_3^-$ content ranges of the pluvial-alluvial fan were 2.24–89.66 mg/L, with an average content of 27.11 mg/L, exceeding China's drinking water standard (Ministry of Health of the PRC and Standardization Administration of the PRC 2006), suggesting great influences of human activities on phreatic water in the pluvial-alluvial fan area, thereby posing certain risks to human health. In contrast, the $NO_3^-$ content ranges in the groundwater of the alluvial plain were 0.00–70.68 mg/L, with an average content of 18.48 mg/L. Although the concentrations of $NO_3^-$ in most water samples did not exceed China's drinking water quality standard, there were some influences of anthropogenic factors on the phreatic water quality (Karagüzel et al. 1998).

The average $F^-$ concentrations in phreatic water were 0.13 and 0.20 mg/L in the upstream and downstream areas, respectively, both of which are within the limits prescribed in the Chinese drinking water quality standard. Indeed, the relatively high pH of phreatic water in the alluvial plain may induce higher concentration of $F^-$ than that in the pluvial-alluvial fan (Currell et al. 2011). This has already been evidenced by a research conducted in an adjacent area (Li et al. 2014b). Fe and Mn contaminations in the phreatic water were relatively serious. The Fe contents in the phreatic water of the pluvial-alluvial fan and alluvial plain were 0.00–1.80 and 0.00–9.60 mg/L, with average contents of 0.19 and 0.84 mg/L, respectively, while the Mn contents in the phreatic water of the pluvial-alluvial fan and alluvial plain were 0.00–462 and 0.00–1417 μg/L, with average contents of 34.02 and 155.92 μg/L, respectively. In the pluvial-alluvial fan, three sampling sites exhibited higher Fe and Mn concentrations than the Chinese drinking water quality standards. Meanwhile, 12 sampling sites in the alluvial plain showed higher Fe and Mn concentrations than the Chinese drinking water quality standards. The average Fe and Mn concentrations in the phreatic water of the alluvial plain were 4.42 and 4.58 times higher than those observed in the pluvial-alluvial fan area, respectively. The higher coefficients of variation indicate a large spatial variation in the Fe and Mn contents. The concentrations of As in groundwater ranged from 1.46 to 7.86 μg/L, which indicated that the concentration of As are within the WHO and Chinese drinking water standards.

The Piper plot for characterizing the hydrochemical facies was also developed in the study (Fig. 3). The obtained results indicated that $HCO_3$-Ca·Mg was the major phreatic water facies type in the pluvial-alluvial fan near the Qinling Mountains. $HCO_3$-Ca·Mg and $SO_4$·Cl-Ca·Mg were the main groundwater facies types in the alluvial plain in the downstream area. These findings demonstrated that carbonate mineral weathering was an important factor controlling phreatic water chemistry, as well as gypsum dissolution to some extent. The calcium carbonate type of groundwater is mainly derived from carbonate mineral dissolution. Indeed, the major minerals in the submerged aquifer of the Wei River Basin are dolomite, calcite, and feldspar (Li et al. 2014b, 2015), which can increase the $Ca^{2+}$, $Mg^{2+}$, and $HCO_3^-$ contents in phreatic water through dissolution processes. However, high $SO_4^{2-}$ and $Cl^-$ contents in phreatic water might be the result of progressive salinization.

The Gibbs diagram (Gibbs 1970) has been utilized in several studies to determine the main factors controlling groundwater chemistry (Marghade et al. 2012). The Gibbs plot for phreatic water in the study area is shown in Fig. 4. Fifty-four water samples were plotted in the rock-dominated areas, and the results showed that water−rock interactions played a decisive role in the phreatic water chemistry in the pluvial-alluvial fan and alluvial plain. The influences of precipitation and evaporation on phreatic water chemistry in the study area were relatively low. Groundwater sampling points located in the alluvial plain were more closely aligned with the evaporation-dominance zone, indicating a strong influence of evaporation on phreatic water chemistry in the alluvial plain, which might be due to the lower groundwater levels in the alluvial plain compared to those in the pluvial-alluvial fan.

## Hydrogeochemical Simulation Along the Groundwater Flow Path

The Gibbs plot and SI indices of major minerals indicated that water−rock interactions were the vital factor controlling groundwater chemistry in the study area. The groundwater residence time and the mineral contents of the aquifer,

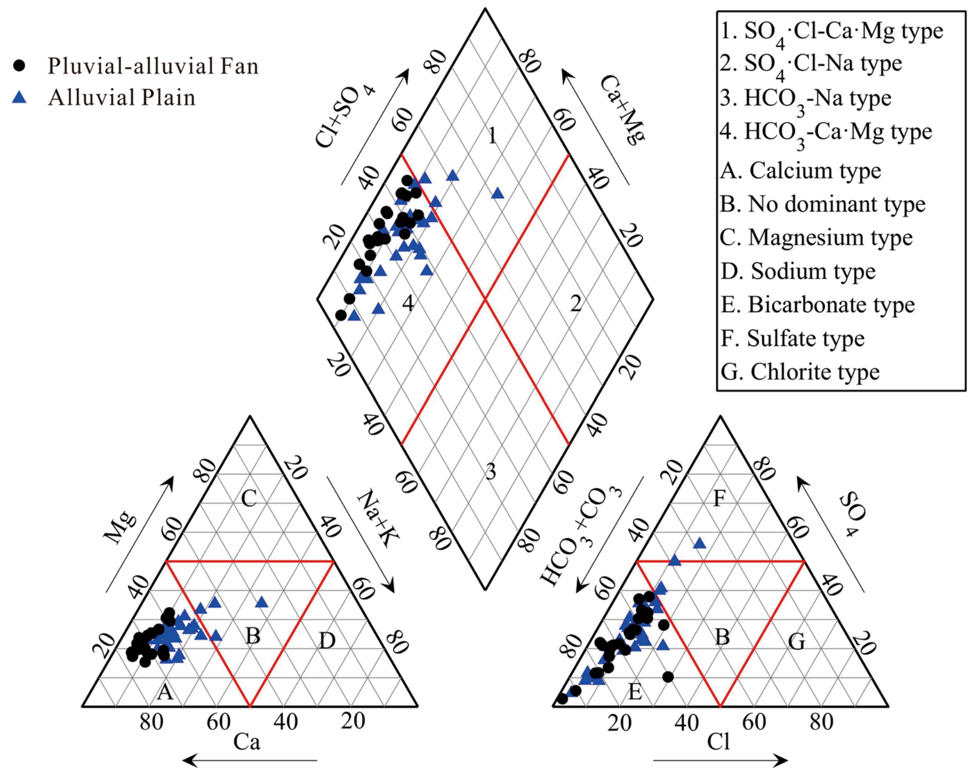


**Fig. 3** Piper diagram showing the hydrochemical characteristics

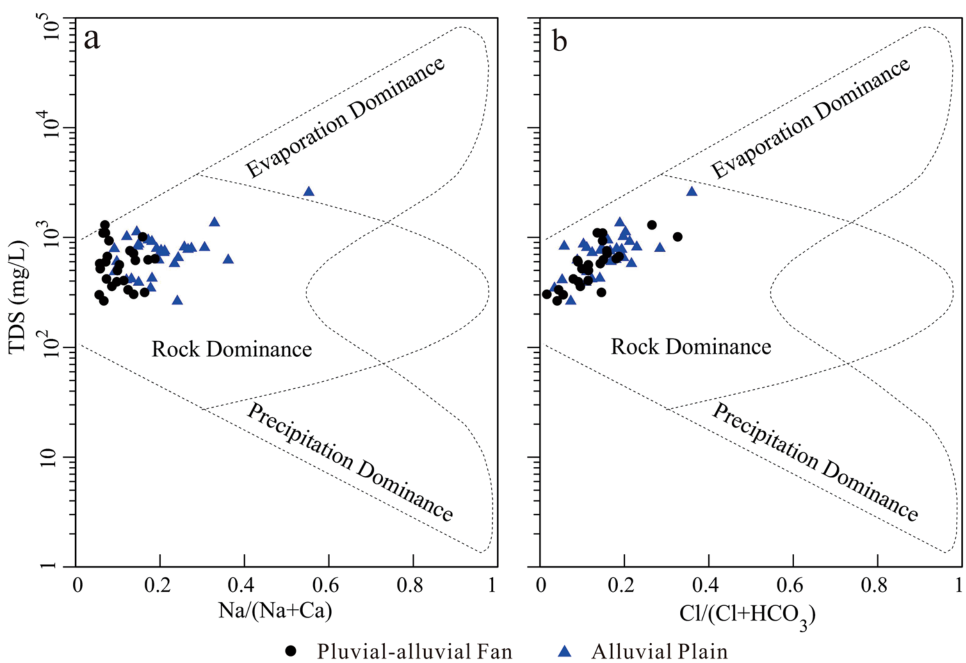


**Fig. 4** Gibbs diagrams indicating general mechanisms of groundwater evolution in the Pluvial-alluvial Fan and Alluvial plain

such as carbonate and silicate, affect the degree of water–rock interactions (Jeong 2001; Wu et al. 2009). Different hydrogeochemical processes in different landscapes result in differences in phreatic water chemistry (Li et al. 2019b). Therefore, in this study, two flow paths were first selected according to the phreatic water flow directions, and then the hydrogeochemical processes were simulated using PHREEQC software. The simulation routes are shown in Fig. 1. Path I is located within Zhouzhi County in the central part of the study area, where the upstream floodplain groundwater flow rates are high, while the phreatic water flow rates downstream are substantially low. Path II is in the eastern part of the study area. Indeed, compared with path I, the phreatic water flow rates in Path II are low without great variations along the path. The main chemical and mineral components in groundwater along flow paths are reported in Table 3 and Table 4.

The PHREEQC simulation results (Table 4) showed that in Path I of the pluvial-alluvial fan (G40-G37) section, there were slight increases in the major anion and cation concentrations. Albite precipitation, halite dissolution, and cation exchange (Eqs. 6 and 7) along Path I are the main processes causing slight increases in the $Na^+$ concentrations in water. The results suggested occurrences of gypsum and fluorite dissolution along Path I, thereby increasing $Ca^{2+}$ concentrations in groundwater. In addition, the increase in $Ca^{2+}$ content also contributed to cation exchange according to Eq. (7). The dissolution of fluorite, halite, gypsum, and calcite along the pathway might also increase the $Cl^-$, $SO_4^{2-}$, and $HCO_3^-$ concentrations in phreatic water. In the section G40-G37, hematite shows precipitation while siderite shows dissolution. Whereas, the amounts of dissolution/precipitation are very small. The presence of $CO_2$(g) in the alluvial plain area downstream of Path I (G37-G36) also enhances dolomite dissolution and gypsum precipitation. The continued dissolution of halite, fluorite, gypsum, and illite and the occurrence of cation exchange (Eqs. 4 and 5) can considerably increase the concentrations of major cations along the flow path. The dissolution of hematite, siderite, and pyrolusite increases the amount of Fe and Mn in groundwater.

$$Mg^{2+}+2NaX \rightarrow MgX_2+2Na^+ \tag{4}$$

$$Ca^{2+}+2NaX \rightarrow CaX_2+2Na^+ \tag{5}$$

$$2Na^+ + MgX_2 \rightarrow 2NaX + Mg^{2+} \tag{6}$$

$$2Na^+ + CaX_2 \rightarrow 2NaX + Ca^{2+} \tag{7}$$

The water−rock interaction in Path II is different from that in Path I. Indeed, $CO_2$ enters the groundwater upstream of Path II (G7-G6), thereby enhancing the dissolution of most minerals except illite and quartz. The dissolution of siderite and pyrolusite increases the Fe and Mn contents in the groundwater. Gypsum and calcite can be precipitated as a result of the continuous groundwater flow through the downstream alluvial plain (G6-G16), reducing the $Ca^{2+}$ and $SO_4^{2-}$ concentrations in groundwater. Dolomite dissolution is the main process increasing the $Mg^{2+}$ concentration in groundwater, while halite dissolution and the exchange of $Na^+$ in submerged aquifers and $Mg^{2+}$ in phreatic water are the principal processes increasing the $Na^+$ concentration. Hematite, siderite, and pyrolusite underwent precipitation, and the Fe and Mn contents were subsequently reduced.

The simulation results showed that water−rock interactions contributed significantly to the major ionic contents of groundwater. Indeed, topographical, hydrological, and geological conditions can considerably affect the water−rock interaction process. The upper section of Path I (G40-G37) is characterized by deep diving depth, steep topography, sand and gravel cobble lithological classes, suitable hydrodynamic environment and runoff conditions, and high diving flow rates, thereby restricting water−rock interaction in the aquifer and, consequently, resulting in low dissolved amounts of minerals. Moreover, the high groundwater level

**Table 4** Possible mineral phase transfer for different pathways calculated by PHREEQC (mmol/L)

| Phrases | Path I | | Path II | |
|---|---|---|---|---|
| | G40-G37 | G37-G36 | G7-G6 | G6-G16 |
| Calcite | 0.252 | − 0.138 | 0.611 | − 1.231 |
| Dolomite | – | 0.356 | 0.244 | 1.383 |
| Fluorite | 0.001 | 0.002 | 0.001 | 0.004 |
| Gypsum | 0.281 | 0.855 | 0.754 | − 4.894 |
| Halite | 0.201 | 0.793 | 0.571 | 0.834 |
| $CO_2$(g) | 0.011 | 0.628 | 1.292 | 1.478 |
| Albite | − 0.041 | − 0.127 | 0.137 | − 0.072 |
| Illite | 0.018 | 0.055 | − 0.060 | 0.031 |
| Quartz | 0.061 | 0.187 | − 0.203 | 0.106 |
| NaX | − 0.089 | 1.595 | − 0.010 | 0.672 |
| CaX | 0.045 | − 0.796 | 0.005 | – |
| MgX | – | – | – | − 0.336 |
| Hematite | − 0.0000772 | 0.0000606 | − 0.005 | − 0.0004 |
| Siderite | 0.000155 | 0.00261 | 0.031 | − 0.0101 |
| Pyrolusite | – | 0.0000729 | 0.008 | − 0.00181 |

**Table 3** Groundwater chemical fraction of different pathways (mg/L)

| Flow path | Sample number | $Na^+$ | $K^+$ | $Ca^{2+}$ | $Mg^{2+}$ | $Cl^-$ | $SO_4^{2-}$ | $HCO_3^-$ | $F^-$ | Fe | Mn | TDS |
|---|---|---|---|---|---|---|---|---|---|---|---|---|
| Path I | G40 | 12.9 | 0.74 | 70.4 | 21.6 | 2.60 | 6.13 | 271 | 0.111 | 0.038 | 0.001 | 303 |
| | G37 | 15.0 | 1.16 | 95.2 | 21.9 | 9.42 | 32.0 | 292 | 0.163 | 0.038 | 0.001 | 410 |
| | G36 | 69.0 | 2.45 | 106 | 31.8 | 37.5 | 114 | 350 | 0.252 | 0.19 | 0.005 | 620 |
| PathII | G7 | 12.9 | 2.45 | 102 | 17.2 | 13.6 | 94.3 | 180 | 0.232 | 0.056 | 0.04 | 499 |
| | G6 | 28.9 | 1.05 | 170 | 21.4 | 33.8 | 176 | 309 | 0.271 | 1.22 | 0.46 | 756 |
| | G16 | 61.8 | 1.78 | 148 | 47.0 | 63.3 | 131 | 453 | 0.426 | 0.61 | 0.36 | 777 |

depths can result in weak evaporation, while the contents of ions along the path increase slightly, with TDS increasing slightly. The G40-G37 section of the aquifer might be dominated by insoluble carbonate or silicate minerals due to long-term leaching (Wang et al. 2009), resulting in extremely low contents of soluble minerals. Thus, the groundwater facies type is Ca·Mg-$HCO_3$. The decrease in the groundwater level depth in the lower part of Path I enhances the evapotranspiration process, while the low topography leads to a subsequent decrease in the hydraulic gradient of groundwater. Furthermore, strong water−rock interactions, low groundwater flow rates, and the poor permeability of the aquifer substantially enhance mineral dissolution, thereby increasing cation and anion concentrations in groundwater to some extent and changing the water chemistry type of groundwater to the Ca-$SO_4$·$HCO_3$ facies type. The changing pattern of anions in groundwater along Path I is consistent with the hydrogeochemical model proposed by Chebotarev et al. (1955).

Path II is characterized by low groundwater depth (less than 10 m), indicating that $CO_2$(g) is mainly involved in water−rock interactions. The low topography and groundwater flow rates in this path are conducive to water−rock interaction, considerably enhancing calcite, dolomite, gypsum, rock salt, and sodium feldspar dissolution in the upper part of Path II compared to those in Path I. The extremely shallow groundwater level depth in the upper section of Path II (less than 3 m) strongly enhances the evaporation process along Path II, thereby substantially increasing the TDS, Fe, and Mn contents in groundwater in this section and resulting in the Ca-$HCO_3$·$SO_4$ facies type of groundwater. Gypsum precipitation in the lower section of Path II results in decreased $Ca^{2+}$ and $SO_4^{2-}$ concentrations in groundwater, thereby changing the groundwater facies type to Ca·Mg-$HCO_3$.

## Distributions of Fe and Mn Concentrations in Phreatic Water and Their Influencing Factors

$NO_3^-$, Fe, and Mn are the main contaminants in the study area, and the distribution of $NO_3$-N in the study area has been studied previously (Xu et al. 2023), so this study focuses on the distribution of Fe and Mn. Fe and Mn are essential trace elements for the human body (Magesh et al. 2017). However, the consumption of water containing high Fe and Mn concentrations exceeding 0.3 and 0.1 mg/L, respectively, may result in the accumulation of trace elements in the body and, consequently, cause various diseases (Sharma et al. 2021). The hydrochemical results of groundwater in the Wei River Basin showed that the Fe and Mn contents in phreatic water exceeded the standard in 25.45 and 20% of the groundwater samples, respectively. The spatial distributions of Fe and Mn concentrations are shown in Fig. 5. The results revealed that the distribution of high value points of Fe in phreatic water in the study area was similar to that of Mn. Water samples with excessive Fe and Mn concentrations were mainly distributed in the alluvial plain, where the lithology is mainly sand, gravel pebbles, and sandy clay. From the perspective of administrative divisions, the high Fe and Mn concentrations in phreatic water were mainly distributed in the entire Huyi District, as well as in some parts of Mei and Zhouzhi counties. The maximum concentration of Fe is 9.6 mg/L, and the maximum concentration of Mn is 1417 μg/L, exceeding China's drinking water standards by 32 and 14 times, respectively.

Previous studies have shown that reducing conditions are favorable for the reduction of high-valent Fe to divalent Fe (Rusydi et al. 2021; Pezzetta et al. 2011). The low-lying terrain, low groundwater runoff, and infiltration of landfill leachate are the main factors enhancing reducing conditions in groundwater (Yuan et al. 2021), which favor the dissolution and enrichment of Fe and Mn in the submerged aquifer in the Huyi District. In addition to the high leaching rates of waste effluent in the district, the widespread distribution of industrial pollution sources might also contribute to the high Fe and Mn concentrations in phreatic water (Sharma et al. 2020; Zhang et al. 2022). Moreover, the redox environment and groundwater flow rates also affect the Fe and Mn concentrations in groundwater. Previous studies have demonstrated that Fe and Mn in groundwater mainly come from mineral dissolution, particularly under low phreatic water flow rates, which are conducive to the dissolution of minerals containing Fe and Mn (Liu et al. 2022). Indeed, the reducing environment and the slow groundwater flow rate promote the elevated Fe and Mn contents in the phreatic water of Huyi District and the alluvial plain.

The correlation coefficients between Fe, Mn, and other major hydrochemical parameters were investigated using Pearson correlation analysis to further reveal the factors affecting the abundance and enrichment of Fe and Mn (Table 5). The chemical properties of Fe and Mn are extremely similar, and both of them are typical redox elements that may change their state of existence under different environmental conditions. Therefore, their levels tend to vary in groundwater. In the study area, Fe showed a positive correlation coefficient of 0.772 with Mn, indicating that these elements in groundwater had similar sources and that their enrichment factors were similar. Fe and Mn were negatively correlated with ORP, with correlation coefficients of −0.492 and −0.666, respectively. McMahon et al. (2008) demonstrated the stability of $NO_3^-$ in an oxidizing environment, indicating that $NO_3$-N concentrations in groundwater are higher in oxidizing environments. The negative correlation coefficients of $NO_3$-N with Fe and Mn in groundwater in the study area were −0.213 and −0.391, respectively, and the $NO_3$-N content in groundwater samples with high Fe

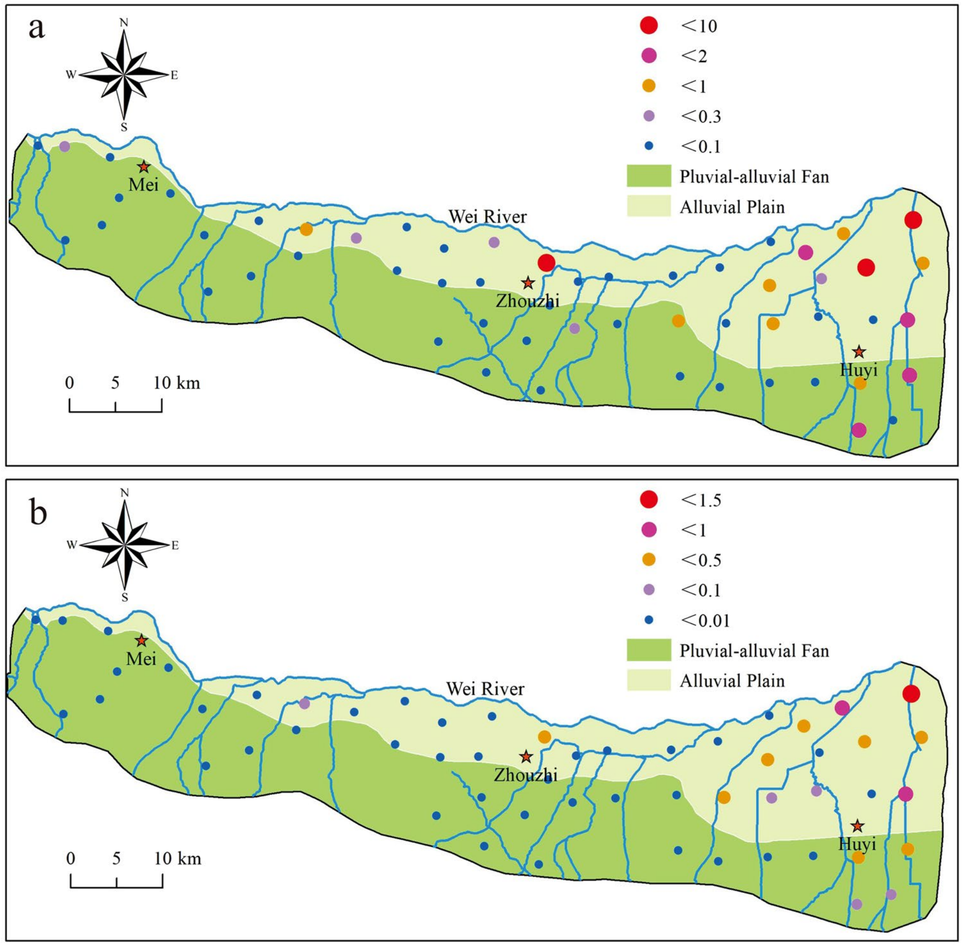


**Fig. 5** Distribution of typical contaminant concentrations in groundwater. **a** Concentration of Fe and **b** Concentration of Mn

**Table 5** Correlation of groundwater Fe and Mn with other physicochemical parameters

| | $NO_3$-N | $Cl^-$ | $SO_4^{2-}$ | $HCO_3^-$ | TDS | ORP | Fe |
|---|---|---|---|---|---|---|---|
| Fe | − 0.213 | 0.692** | 0.818** | 0.520** | 0.634** | − 0.492** | 1.000 |
| Mn | − 0.391** | 0.687** | 0.824** | 0.540** | 0.549** | − 0.666** | 0.722** |

**Indicates correlation significance at the 0.01 level (two-tailed), and *means correlation significance at the 0.05 level (two-tailed)

and Mn contents tended to be smaller, suggesting a reducing environment for groundwater. This further indicates that the reducing environment is one of the factors affecting the Fe and Mn enrichment in groundwater in the study area. Debye-Hückel's theory suggests that high TDS contents lead to lower ionic activity coefficients, thereby increasing the dissolved Fe and Mn concentrations (Zhang et al. 2020b). Fe and Mn concentrations exhibited significant positive correlation coefficients with TDS of 0.634 and 0.549, respectively, indicating that the Fe and Mn enrichment in the phreatic water was also influenced by high TDS contents. The high contents of anions (e.g., $HCO_3^-$, $SO_4^{2-}$, and $Cl^-$) in phreatic water can also enhance the dissolution of Fe and Mn, resulting in their enrichment in the water, which is demonstrated by the positive correlation of Fe and Mn contents with $Cl^-$, $SO_4^{2-}$, and $HCO_3^-$. The research results of Rusydi et al. (2021) have proven that inorganic complexes promote the dissolution of Fe and Mn.

## Stochastic Health Risks in Phreatic Water

The deterministic health risk of $NO_3$-N has been reported by Xu et al. (2023). However, the stochastic health risk of it was never reported in the study area. Therefore, the stochastic health risks of $NO_3$-N, Fe, and Mn were assessed using Monte Carlo methods, and the results of the non-carcinogenic risks of $NO_3$-N, Fe, and Mn for adults and children in the study area are shown in Fig. 6a–h. The total non-carcinogenic risk for $NO_3$-N, Fe, and Mn for adults was 0.06–1.19 (at the 95% confidence level) with a mean

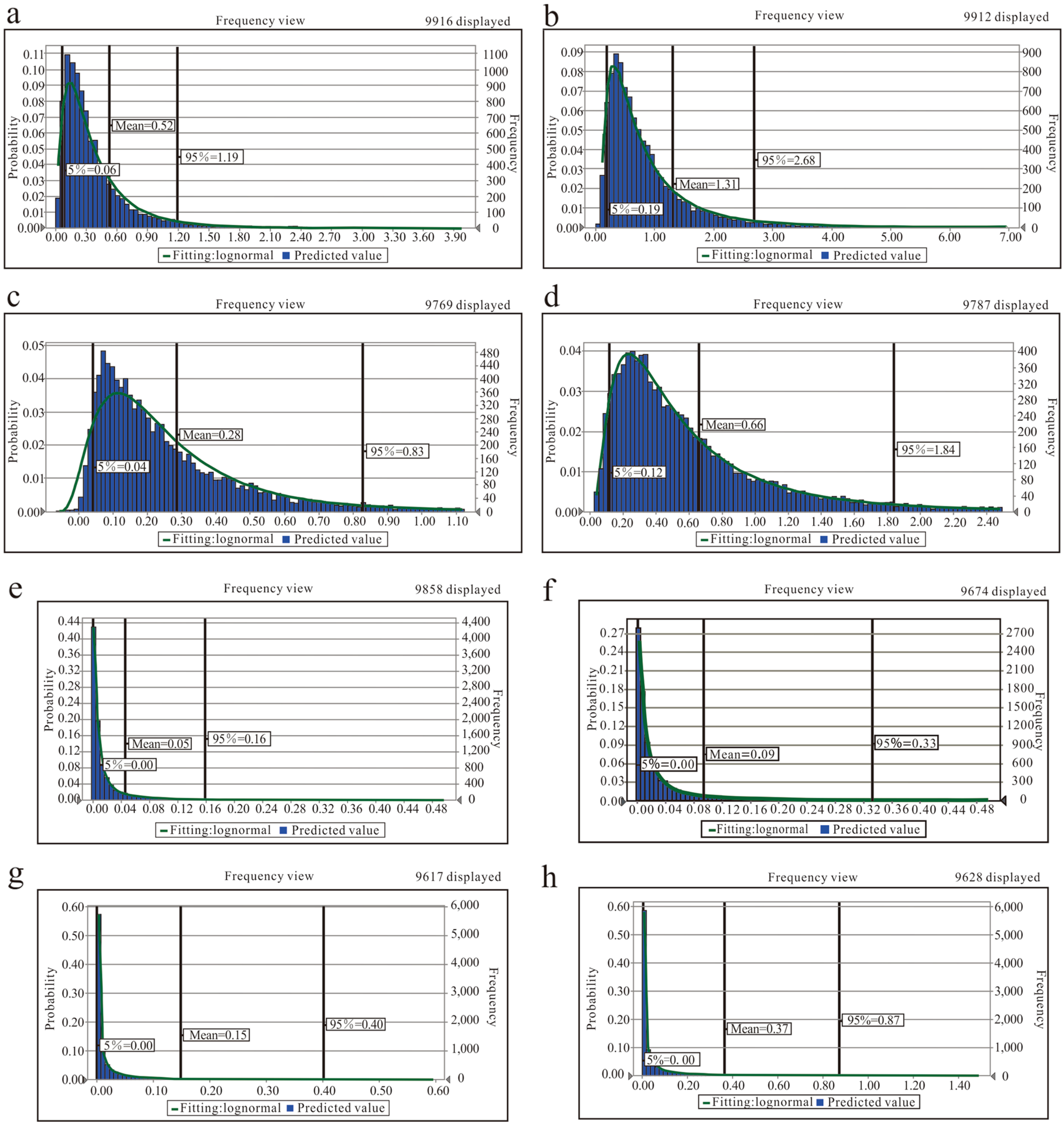


**Fig. 6** Plots of **a** total non-carcinogenic risk for adults **b** total non-carcinogenic risk for children **c** non-carcinogenic risk of $NO_3$-N for adults **d** non-carcinogenic risk of $NO_3$-N for children **e** non-carcinogenic risk of Fe for adults **f** non-carcinogenic risk of Fe for children **g** non-carcinogenic risk of Mn for adults and **h** non-carcinogenic risk of Mn for children

value of 0.52 and a probability of causing a health hazard of 7.2%. The total non-carcinogenic risk range for $NO_3$-N, Fe, and Mn for children was 0.19–2.68 (at the 95% confidence level), with a mean value of 1.31 and a 28.5% probability of causing a health hazard. Among them, $NO_3$-N poses the greatest health risk to the population, causing a health risk probability of 3.1% and 18.3%, respectively. The health risk probabilities of Mn for adults and children were 2.3% and 4.9%, respectively, with mean values of 0.15 and 0.37. Fe posed the lowest health risk to the local population with mean values of 0.05 and 0.09 for adults and children, respectively, causing a very small probability of health risk. The probability of the non-carcinogenic health risk for children was higher than that for adults. Monte Carlo simulations showed that $NO_3$-N and Mn were the main contaminants that contributed to health risks for different age groups in the study area. Particularly, the area with the highest probability of health risk due to Mn was the Huyi District, where groundwater Mn concentrations are generally high. This finding is, indeed, consistent with previous related research reports (Ahmed et al. 2019; Sharma et al. 2021; Liu et al. 2022).

Studies on the hazards of $NO_3^-$, Fe, and Mn in humans have shown that high concentrations of $NO_3^-$ can cause toxicity, and that the accumulation of Mn may cause Parkinson's disease in adults, endanger adult mental health, and affect the intelligence quotient (IQ) of children and their learning ability (Frisbie et al. 2012; Farina et al. 2013). Therefore, the outcome of Monte Carlo evaluation shows that it is important to treat phreatic water with high $NO_3^-$, Fe, and Mn contents before its use for drinking purposes. Particular attention needs to be paid to the potential health problems for children in the Huyi District, where high groundwater $NO_3^-$, Fe and Mn concentrations have been observed.

## Conclusions

This study investigated the characterization of hydrochemical changes along the phreatic water flow direction, as well as Fe, $NO_3^-$ and Mn-associated human health risks, in the rural areas of the Wei River Basin, China. In addition, the distribution of Fe and Mn in the Wei River Basin and its influencing factors are discussed in this study. The following research findings were obtained:

- In the pluvial-alluvial fan and alluvial plan, the abundance of cations followed the order of $Ca^{2+} > Mg^{2+} > Na^+ > K^+$ and $Ca^{2+} > Na^+ > Mg^{2+} > K^+$, respectively. Water−rock interaction is the key factor influencing groundwater chemistry in the Wei River Basin. In addition, the groundwater chemical types of the pluvial-alluvial fan are all $HCO_3$-Ca·Mg facies types, while 86.67% of the groundwater chemical types of the alluvial plain are $HCO_3$-Ca·Mg facies types. Twelve percent and 40% of groundwater samples in the pluvial-alluvial fan and alluvial plain, respectively, exhibited high Fe and Mn concentrations, exceeding China's drinking water standards.
- The simulation results indicated fluorite, gypsum, halite, illite, siderite, and pyrolusite dissolution along Path I, while albite precipitation was observed along path I. The exchange of $Na^+$ in groundwater with $Ca^{2+}$ in the upper section was replaced with the exchange of $Ca^{2+}$ in groundwater with $Na^+$ in the aquifer. In path II, the dissolution of gypsum, dolomite, siderite, and pyrolusite occurs in the upstream (G7−G6) and turns to precipitation in the downstream area (G6−G16). The differences between the two flow paths in water−rock interaction might be due to the different groundwater flow rates, groundwater levels, geological conditions, and hydrogeological conditions.
- The spatial distribution patterns of groundwater Fe and Mn contents in the Wei River Basin were similar. Higher Fe and Mn contents were noted in the eastern part of the study area (the Huyi District) and in some parts of Zhouzhi County and Mei County. The low ORP, low phreatic water flow rates, and high TDS contents might contribute to Fe and Mn enrichment in phreatic water. Moreover, sewage infiltration from industries and landfills may also contribute to high phreatic water Fe and Mn concentrations.
- The probability of health risk from $NO_3$-N, Fe, and Mn is 7.2% for adults and 28.5% for children. The main contaminants that pose health risks to the population are $NO_3$-N and Mn, with the probability of health risks for children and adults being 18.3% and 3.1% for $NO_3$-N, and 4.9% and 2.3% for Mn, respectively. The health risk of Fe to the local population is negligible. Therefore, it is necessary to ensure safe drinking water to reduce the health risk induced by $NO_3$-N and Mn in the Wei River Basin.

**Acknowledgements** We are grateful for the useful comments and suggestions rendered by the editors and reviewers, which are essential for us to further improve the quality of the manuscript.

**Author Contributions** WG participated in the field work, developed the methodologies involved in this research and wrote the early version of the manuscript. PL developed the core idea of conducting this research, participated in field investigation and supervised the entire research. He also participated in writing the early version and reviewed and edited all versions of the manuscript. QD and YZ participated in the field investigation and sample collection, participated in the writing of the early version of the manuscript and reviewed the revised version of the manuscript. DX and ZZ were involved in the research design, participated in the discussion on the research contents, and reviewed the revised version of the manuscript.

**Funding** Financial support from the National Natural Science Foundation of China (42072286 and 41761144059), the Qinchuangyuan "Scientist + Engineer" Team Development Program of the Shaanxi Provincial Department of Science and Technology (2022KXJ-005), the Fok Ying Tong Education Foundation (161098), and the National Ten Thousand Talent Program (W03070125) is acknowledged.

**Data Availability** All the raw data may be provided upon reasonable request.

## Declarations

**Conflicts of interest** All authors of this article declare that they have no known conflicts of interest.

## References


Ahmed N, Bodrud-Doza M, Towfiqul Islam ARM, Hossain S, Moniruzzaman M, Deb N, Bhuiyan MAQ (2019) Appraising spatial variations of As, Fe, Mn and NO3 contaminations associated health risks of drinking water from Surma basin, Bangladesh. Chemosphere 218:726–740. https://doi.org/10.1016/j.chemosphere.2018.11.104

Banerjee A, Singh P, Pratap K (2016) Hydrogeological component assessment for water resources management of semi-arid region: a case study of Gwalior M.P., India. Arab J Geosci 9(18):1–13. https://doi.org/10.1007/s12517-016-2736-8

Chakraborty B, Roy S, Bera B, Adhikary P, Bhattacharjee S, Sengupta D, Shit P (2022) Evaluation of groundwater quality and its impact on human health: a case study from Chotanagpur plateau fringe region in India. Appl Water Sci 12(3):25. https://doi.org/10.1007/s13201-021-01539-6

Chebotarev II (1955) Metamorphism of natural waters in the crust of weathering-1. Geochimica Cosmochimica Acta 8(1–2):22–48. https://doi.org/10.1016/0016-7037(55)90015-6

Chen J, Gao Y, Qian H, Ren W, Qu W (2021) Hydrogeochemical evidence for fluoride behavior in groundwater and the associated risk to Human health for a large irrigation plain in the Yellow River Basin. Sci Total Environ 800:149428. https://doi.org/10.1016/j.scitotenv.2021.149428

Currell M, Cartwright I, Raveggi M, Han DM (2011) Controls onelevated fluoride and arsenic concentrations in groundwater fromthe Yuncheng Basin. China Appl Geochem 26(4):540–552. https://doi.org/10.1016/j.apgeochem.2011.01.012

Dragon K, Jozef G (2009) Dentifcation of hydrogeochemical zones in postglacial buried valley aquifer Wielkopolska Buried Valley aquifer. Poland Environ Geol 58:859–866. https://doi.org/10.1007/s00254-008-1561-0

Farina M, Avila D, da Rocha J, Aschner M (2013) Metals, oxidative stress and neurodegeneration: a focus on iron, manganese and mercury. Neurochem Int 62(5):575–594. https://doi.org/10.1016/j.neuint.2012.12.006

Fathy I, Ahmed A, Abd-Elhamid H (2021) Integrated management of surface water and groundwater to mitigate flood risks and water scarcity in arid and semi-arid regions. J Flood Risk Manag 14(3):e12720. https://doi.org/10.1111/jfr3.12720

Frisbie S, Mitchell E, Dustin H, Maynard D, Sarkar B (2012) World Health Organization discontinues its drinking-water guideline for manganese. Environ Health Perspect 120(6):775–778. https://doi.org/10.1289/ehp.1104693

Ganyaglo S, Gibrilla A, Teye E, Owusu-Ansah E, Tetty S, Diabene P, Asimah S (2019) Groundwater fluoride contamination and probabilistic health risk assessment in fluoride endemic areas of the Upper East Region, Ghana. Chemosphere 233:862–872. https://doi.org/10.1016/j.chemosphere.2019.05.276

Gibbs R (1970) Mechanisms controlling world water chemistry. Science 170(3962):1088–1090. https://doi.org/10.1126/science.170.3962.1088

Guo Y, Li P, He X, Wang L (2022) Groundwater quality in and around a Landfill in Northwest China: characteristic pollutant identification, health risk assessment, and controlling factor analysis. Expo Health 14(4):885–901. https://doi.org/10.1007/s12403-022-00464-6

Hafeman D, Factor-Litvak P, Cheng Z, van Geen A, Ahsan H (2007) Association between manganese exposure through drinking water and infant mortality in Bangladesh. Environ Health Perspect 115(7):1107–1112. https://doi.org/10.1289/ehp.10051

He X, Li P, Ji Y, Wang Y, Su Z, Elumalai V (2020) Groundwater arsenic and fluoride and associated arsenicosis and fluorosis in China: occurrence distribution and management. Expo Health 12(3):355–368. https://doi.org/10.1007/s12403-020-00347-8

Jeong C (2001) Effect of land use and urbanization on hydrochemistry and contamination of groundwater from Taejon area. Korea J Hydrol 253(1–4):194–210. https://doi.org/10.1016/S0022-1694(01)00481-4

Jha SK, Nayak AK, Sharma YK, Sharma DK, Mishra VK (2015) Assessing seasonal variation of fluoride in groundwater for irrigation uses through hydrogeochemical and multivariate statistical approach. Toxicol Environ Chem 97(7):868–887. https://doi.org/10.1080/02772248.2015.1070532

Jing X, Yang H, Cao Y, Wang W (2014) Identification of indicators of groundwater quality formation process using a zoning model. J Hydrol 514:30–40. https://doi.org/10.1016/j.jhydrol.2014.03.059

Karagüzel R, Irlayici A (1998) Groundwater pollution in the Isparta Plain. Turkey Environ Geol 34(4):303–308. https://doi.org/10.1007/s002540050282

Kshetrimayum K, Hegeu H (2016) The state of toxicity and cause of elevated iron and manganese concentrations in surface water and groundwater around naga thrust of Assam-Arakan basin Northeastern India. Environ Earth Sci 75(7):604. https://doi.org/10.1007/s12665-016-5372-4

Kurwadkar S (2019) Occurrence and distribution of organic and inorganic pollutants in groundwater. Water Environ Res 91(10):1001–1008. https://doi.org/10.1002/wer.1166

Li P, Qian H, Wu J, Ding J (2010) Geochemical modeling of groundwater in southern plain area of Pengyang County, Ningxia. China Water Sci Eng 3(3):282–291. https://doi.org/10.3882/j.issn.1674-2370.2010.03.004

Li L, Wang Y, Wu Y, Li J (2013) Major geochemical controls on fluoride enrichment in groundwater: a case study at datong basin, Northern China. J Earth Sci 24(6):976–986. https://doi.org/10.1007/s12583-013-0385-3

Li P, Wu J, Qian H, Lyu X, Liu H (2014a) Origin and assessment of groundwater pollution and associated health risk: a case study in an industrial park, northwest China. Environ Geochem Health 36(4):693–712. https://doi.org/10.1007/s10653-013-9590-3

Li P, Qian H, Wu J, Chen J, Zhang Y, Zhang H (2014b) Occurrence and hydrogeochemistry of fluoride in alluvial aquifer of Weihe River. China Environ Earth Sci 71(7):3133–3145. https://doi.org/10.1007/s12665-013-2691-6

Li P, Wu J, Qian H (2015) Hydrochemical appraisal of groundwater quality for drinking and irrigation purposes and the major influencing factors: a case study in and around Hua County. China Arab J Geosci 9(1):15. https://doi.org/10.1007/s12517-015-2059-1

Li P, Wu J, Qian H (2016a) Preliminary assessment of hydraulic connectivity between river water and shallow groundwater and estimation of their transfer rate during dry season in the Shidi River. China Environ Earth Sci 75(2):99–116. https://doi.org/10.1007/s12665-015-4949-7

Li P, Wu J, Qian H, Zhang Y, Yang N, Jing L, Yu P (2016b) Hydrogeochemical characterization of groundwater in and around a wastewater irrigated forest in the Southeastern Edge of the Tengger Desert Northwest China. Expo Health 8(3):331–348. https://doi.org/10.1007/s12403-016-0193-y

Li P, He X, Guo W (2019a) Spatial groundwater quality and potential health risks due to nitrate ingestion through drinking water: a case study in Yan'an City on the Loess Plateau of northwest China. Hum Ecol Risk Assess 25(1–2):11–31. https://doi.org/10.1080/10807039.2018.1553612

Li M, Liang X, Xiao C, Cao Y, Hu S (2019b) Hadrochemical evolution of groundwater in a typical semi-arid groundwater storage basin using a zoning model. Water 11(7):1334. https://doi.org/10.3390/w11071334

Li Y, Li P, Cui X, He S (2021) Groundwater quality, health risk, and major influencing factors in the lower Beiluo River watershed of northwest China. Hum Ecol Risk Assess 27(7):1987–2013. https://doi.org/10.1080/10807039.2021.1940834

Liu L, Wu J, He S, Wang L (2022) Occurrence and distribution of groundwater fluoride and manganese in the Weining Plain (China) and their probabilistic health risk quantification. Expo Health 14(2):263–279. https://doi.org/10.1007/s12403-021-00434-4

Ma B, Jin M, Liang X, Li J (2018) Groundwater mixing and mineralization processes in a mountain-oasis-desert basin, northwest China: hydrogeochemistry and environmental tracer indicators. Hydrogeol J 26(1):233–250. https://doi.org/10.1007/s10040-017-1659-0

Magesh N, Chandrasekar N, Elango L (2017) Trace element concentrations in the groundwater of the Tamiraparani river basin, South India: insights from human health risk and multivariate statistical techniques. Chemosphere 185:468–479. https://doi.org/10.1016/j.chemosphere.2017.07.044

Marghade D, Malpe DB, Zade AB (2012) Major ion chemistry of shallow groundwater of a fast growing city of central India. Environ Monit Assess 184(4):2405–2418. https://doi.org/10.1007/s10661-011-2126-3

McMahon P, Chapelle F (2008) Redox processes and water quality of selected principal aquifer systems. Groundwater 46(2):259–271. https://doi.org/10.1111/j.1745-6584.2007.00385.x

Ministry of Environmental Protection of the P.R. China (2019) Technical guidelines for risk assessment of soil contamination of land for construction (HJ 25.3-2019). China Environmental Science Press, Beijing

Ministry of Environmental Protection of the P.R. China (2020) Technical specifications for environmental monitoring of groundwater (HJ/T 164–2020). China Environmental Science Press, Beijing

Ministry of Health of the PRC, Standardization Administration of the PRC (2006) Standards for drinking water quality (GB 5749–2006). China Standard Press, Beijing

Natesan D, Sabarathinam C, Kamaraj P, Mathivanan M, Haji M, Viswanathan P, Chandrasekaran T, Rajendran T (2022) Impact of monsoon shower on the hydrogeochemistry of groundwater along the lithological contact: a case study from South India. Appl Water Sci 12(3):36. https://doi.org/10.1007/s13201-021-01538-7

Pezzetta E, Lutman A, Martinuzzi I, Viola C, Bernardis G, Fuccaro V (2011) Iron concentrations in selected groundwater samples from the lower Friulian Plain, northeast Italy: importance of salinity. Environ Earth Sci 62(2):377–391. https://doi.org/10.1007/s12665-010-0533-3

Poetra R, Adji T, Santosa L, Khakhim N (2020) Hydrogeochemical conditions in groundwater systems with various geomorphological units in Kulonprogo Regency, Java Island. Indonesia Aquat Geochem 26(4):421–454. https://doi.org/10.1007/s10498-020-09384-w

Ren X, Li P, He X, Su F, Elumlai V (2021) Hydrogeochemical processes affecting groundwater chemistry in the central part of the Guanzhong Basin. China Arch Environ Contam 80(1):74–91. https://doi.org/10.1007/s00244-020-00772-5

Rusydi A, Onodera SI, Saito M, Ioka S, Maria R, Ridwansyah I, Delinom R (2021) Vulnerability of groundwater to iron and manganese contamination in the coastal alluvial plain of a developing Indonesian city. SN Appl Sci 3(4):399. https://doi.org/10.1007/s42452-021-04385-y

Rutchik J, Zheng W, Jiang Y, Mo X (2012) How does an occupational neurologist assess welders and steelworkers for a manganese-induced movement disorder? An international team's experiences in Guangxi, China. Part II Occup Environ Med 54(12):1562–1564. https://doi.org/10.1097/JOM.0b013e318216d01b

Schlager E (2006) Challenges of governing groundwater in U.S. western states. Hydrogeol J 14(3):350–360. https://doi.org/10.1007/s10040-005-0012-1

Sharma A, Ganguly R, Gupta A (2020) Impact assessment of leachate pollution potential on groundwater: an indexing method. J Environ Eng 146(3):05019007. https://doi.org/10.1061/(ASCE)EE.1943-7870.0001647

Sharma G, Jena R, Ray P, Yadav K, Moharana P, Cabral-Pinto M, Bordoloi G (2021) Evaluating the geochemistry of groundwater contamination with iron and manganese and probabilistic human health risk assessment in endemic areas of the world's largest River Island India. Environ Toxicol Pharmacol 87:103690. https://doi.org/10.1016/j.etap.2021.103690

Singh PK, Verma P, Tiwari AK (2018) Hydrogeochemical investigation and qualitative assessment of groundwater resources in Bokaro district, Jharkhand. India Arab J Geosci 11(17):483. https://doi.org/10.1007/s12517-018-3831-9

Snousy M, Wu J, Su F, Abdelhalim A, Ismail E (2022) Groundwater quality and its regulating geochemical processes in Assiut Province. Egypt Expo Health 14(2):305–323. https://doi.org/10.1007/s12403-021-00445-1

Su Z, Wu J, He X, Elumlai V (2020) Temporal changes of groundwater quality within the groundwater depression cone and prediction of confined groundwater salinity using grey markov model in Yinchuan Area of Northwest China. Expo Health 12:447–468. https://doi.org/10.1007/s12403-020-00355-8

Touhari F, Meddi M, Mehaiguene M, Razack M (2015) Hydrogeochemical assessment of the Upper Cheliff groundwater (North West Algeria). Environ Earth Sci 73(7):3043–3061. https://doi.org/10.1007/s12665-014-3598-6

Wang Y, Shvartsev S, Su C (2009) Genesis of arsenic/fluoride-enriched soda water: a case study at Datong, northern China. Appl Geochem 24(4):641–64912. https://doi.org/10.1016/J.APGEOCHEM.2008.12.015

Wang L, Li P, Duan R, He X (2022) Occurrence, controlling factors and health risks of $Cr^{6+}$ in groundwater in the guanzhong Basin of China. Expo Health 14:239–251. https://doi.org/10.1007/s12403-021-00410-y

Wei M, Wu J, Li W, Zhang Q, Su F, Wang Y (2022) Groundwater geochemistry and its impacts on groundwater arsenic enrichment, variation, and health risks in Yongning County, Yinchuan Plain of Northwest China. Expo Health 14(2):219–238. https://doi.org/10.1007/s12403-021-00391-y

Wu J, Sun Z (2016) Evaluation of shallow groundwater contamination and associated human health risk in an alluvial plain impacted by agricultural and industrial activities. Mid-West China Expo Health 8(3):311–329. https://doi.org/10.1007/s12403-015-0170-x

Wu P, Tang C, Zhu L, Liu C, Cha X, Tao X (2009) Hydrogeochemical characteristics of surface water and groundwater in the karst basin, southwest China. Hydrol Process 23(14):2012–2022. https://doi.org/10.1002/hyp.7332

Wu J, Zhang Y, Zhou H (2020) Groundwater chemistry and groundwater quality index incorporating health risk weighting in Dingbian County, Ordos Basin of Northwest China. Geochemistry 80(4):125607. https://doi.org/10.1016/j.chemer.2020.125607

Xu P, Feng W, Qian H, Zhang Q (2019) Hydrogeochemical characterization and irrigation quality assessment of shallow groundwater in the central-Western Guanzhong Basin, China. Int J Env Res Pub He 16(9):1492. https://doi.org/10.3390/ijerph16091492

Xu D, Li P, Chen X, Yang S, Zhang P, Guo F (2023) Major ion hydrogeochemistry and health risk of groundwater nitrate in selected rural areas of the Guanzhong Basin, China. Hum Ecol Risk Assess. https://doi.org/10.1080/10807039.2022.2164246

Yadav K, Kumar S, Pham Q, Gupta N, Rezania S, Kamyab H, Yadav S, Vymazal J, Kumar V, Tri D (2019) Fluoride contamination, health problems and remediation methods in Asian groundwater: comprehensive review. Ecotoxicol Environ Saf 182:109362. https://doi.org/10.1016/j.ecoenv.2019.06.045

Yuan R, Zhang L, Long X (2021) Iron and manganese contamination of shallow groundwater in the upper plains of Dongting Lake. Journal of China Hydrology 41(5):97–102 ((**in Chinese**))

Zhang C, Wei Z, Sun Y, Li H, Wang W, Duan L (2013) Evolutionary mechanism of diving hydrogeochemistry in the Guanzhong Basin. South-to-North Water Transfers and Water Science & Technology 11(05):48–52 ((**in Chinese**))

Zhang X, Miao J, Hu B, Liu H, Zhang H, Ma Z (2017) Hydrogeochemical characterization and groundwater quality assessment in intruded coastal brine aquifers (Laizhou Bay, China). Environ Sci Pollut Res 24(26):21073–21090. https://doi.org/10.1007/s11356-017-9641-x

Zhang Y, Xu B, Guo Z, Han J, Li H, Jin L, Chen F, Xiong Y (2019a) Human health risk assessment of groundwater arsenic contamination in Jinghui irrigation district, China. J Environ Manage 237:163–169. https://doi.org/10.1016/j.jenvman.2019.02.067

Zhang F, Huang G, Hou Q, Liu C, Zhang Y, Zhang Q (2019b) Groundwater quality in the Pearl River Delta after the rapid expansion of industrialization and urbanization: Distributions, main impact indicators and driving forces. J Hydrol 577:124004. https://doi.org/10.1016/j.jhydrol.2019.124004

Zhang Q, Xu P, Qian H (2019c) Assessment of groundwater quality and human health risk (HHR) evaluation of nitrate in the central-western Guanzhong Basin, China. Int J Env Res Pub He 16(21):4246. https://doi.org/10.3390/ijerph16214246

Zhang Q, Xu P, Qian H, Yang F (2020a) Hydrogeochemistry and fluoride contamination in Jiaokou Irrigation District, Central China: Assessment based on multivariate statistical approach and Human health risk. Sci Total Environ 741:140460. https://doi.org/10.1016/j.scitotenv.2020.140460

Zhang Z, Xiao C, Adeyeye O, Yang W, Liang X (2020b) Source and mobilization mechanism of iron, manganese and arsenic in groundwater of Shuangliao City. Northeast China Water 12(2):534. https://doi.org/10.3390/w12020534

Zhang Q, Li P, Lyu Q, Ren X, He S (2022) Groundwater contamination risk assessment using a modified DRATICL model and pollution loading: A case study in the Guanzhong Basin of China. Chemosphere 291. https://doi.org/10.1016/j.chemosphere.2021.132695

**Publisher's Note** Springer Nature remains neutral with regard to jurisdictional claims in published maps and institutional affiliations.